# Crystal growth and characterization of the cubic semiconductor $Cu_2SnSe_4$

G. Marcano,[a] C. Rincón, G. Marín, and R. Tovar
*Departamento de Física, Facultad de Ciencias, Centro de Estudios de Semiconductores, Universidad de Los Andes, Mérida 5101, Venezuela*

G. Delgado
*Laboratorio de Cristalografía, Departamento de Química, Facultad de Ciencias, Universidad de Los Andes, Mérida 5101, Venezuela*

(Received 5 March 2002; accepted for publication 15 May 2002)

X-ray powder diffraction study of the *p*-type semiconductor $Cu_2SnSe_4$ shows that this material crystallizes in the cubic structure, space group $F\bar{4}3m$, with unit cell parameter $a=5.6846(3)$ Å. The temperature variation of the hole concentration between 120 and 300 K, obtained from the Hall effect and electrical resistivity measurements, is due to the thermal activation of an acceptor level with ionization energy of about 0.02 eV. The temperature variation of the hole mobility is explained by considering the scattering of charge carriers by ionized impurities and acoustic phonons. From this analysis, the density-of-states effective mass of the holes is estimated to be about 0.8 $m_e$, $m_e$ being the free electron effective mass. From the optical absorption spectra, the fundamental absorption edge is found to be direct. The value of the lowest energy gap and the spin-orbit splitting were estimated to be about 0.35 and 0.20 eV, respectively. The temperature dependence of the magnetization measurements shows that $Cu_2SnSe_4$ is paramagnetic, indicating that most of the copper atoms have the divalent charge state. © *2002 American Institute of Physics.*
[DOI: 10.1063/1.1492018]

## I. INTRODUCTION

The low-melting point $A_2^IB^{IV}C_3^{VI}$ ternary compounds[1] are of considerable interest[2–8] as potential small band-gap semiconductors for electro-optic devices.[2] One of them, $Cu_2SnSe_3$, which crystallizes in a monoclinic structure[7,8] could be used for acousto-optic applications[6,7] in the infrared region around 0.8 eV. However, as in the case of most of the $A_2^IB^{IV}C_3^{VI}$ semiconductors, the preparation of homogeneous crystals of this compound is not easy and deviation from the ideal composition is observed in samples prepared from different conventional crystal growth techniques. In an attempt to improve the quality of the synthesized crystals, ingots with slight deviations from the ideal stoichiometry were prepared from the melt. Se-rich crystals thus obtained, as analyzed by x-ray powder diffraction (XRD) and energy dispersive x-ray (EDX) spectroscopy, show a cubic crystalline structure and compositions of Cu:Sn:Se very close to 2:1:4, respectively. This indicates the formation of $Cu_2SnSe_4$ crystals. The compound $Cu_2SnSe_4$, or more precisely $Cu_2Sn\square Se_4$, where $\square$ denotes the cation vacancy which is included to maintain the same number of cations and anions sites, belongs to one of the families of fourfold defect derivative of the $A^{II}B^{VI}$ binary semiconductors.[9] It is expected, in order to maintain an average of four valence electrons per lattice site, that copper atoms should be divalent ($Cu^{2+}$) in $Cu_2SnSe_4$.

The crystal structure of $Cu_2SnSe_4$ was earlier reported by Bok and De Witt[10] (Joint Committee on Powder Diffraction Standards No. 16-0670). They found that this material crystallizes in the cubic structure, space group $F\bar{4}3m$, with lattice parameter $a=5.690(2)$ Å. More recently,[11,12] analysis of XRD patterns of nanocrystals of $Cu_2SnSe_4$, synthesized through solvothermal process, also indicates that the compound crystallizes in a cubic structure with lattice constant $a=5.712$ Å. [11] In this article we report on the growth, crystal structure, electrical, optical, and magnetic characterization of $Cu_2SnSe_4$. The study shows that this material is a *p*-type cubic semiconductor and presents a direct band gap.

## II. EXPERIMENTAL DETAILS

Ingots of $Cu_2SnSe_4$ were prepared from the melt by the vertical Bridgman–Stockbarger technique. They were obtained by heating the mixture of Cu, Sn and Se, in the proportion 2:1:4 sealed in evacuated quartz ampoules. The ampoules were placed in a multiple zone vertical furnace. Initially they were heated from room temperature to 1150 °C at a rate of 40 °C/h. The molten mixture was kept at this temperature for 24 h. In order to assure a homogeneous mixing, the ampoule was agitated periodically. It was later cooled at a rate of 10 °C/h up to 800 °C, then at 1 °C/h to 640 °C. The cooling rate from 640 to 500 °C was 5 °C/h. The ingots were annealed at this temperature for 120 h. The furnace was then turned off and the ingot cooled down to room temperature.

The chemical analysis of samples taken from the central part of the ingots was performed by EDX using a Kevex model Delta-3 system connected to a Hitachi model S-2500

[a]Electronic mail: gmarcano@ciens.ula.ve

 

scanning electron microscope (SEM). The error in standardless analysis was around 5%.

X-ray powder diffraction (XRD) data were collected at room temperature in reflection mode using a Siemens D5005 diffractometer equipped with a Cu-target tube and a diffracted beam graphite monochromator. A fixed aperture and divergence slit of 1 mm, a 0.1 mm monochromator slit, and 0.6 mm detector slit were used. The specimen was scanned in the $2\theta$ range of 20°–120°, the scan step was 0.02°, and the time of counting in every step was 45 s. Quartz was used as an external standard. Precise determination of the peak positions was performed using conventional analytical software.

The hole concentration $p$ and Hall mobility $\mu$ in the temperature range from 77 to 300 K were determined by combined Hall effect and conductivity measurements made by the four point probe standard technique. In-soldered contacts were made by etching the sample's surface with a low melting point solder flux using a low power iron solder. The contacts were ohmic in the temperature range of interest. A magnetic field of 10 KG was employed in the Hall measurements.

The absorption coefficient spectra at room temperature in the energy range from 0.1 to 1.0 eV was obtained using a Perkin-Elmer Fourier transform infrared (FTIR) spectrometer model 1725X.

The magnetic properties were studied in the temperature range from 5 to 300 K by magnetization measurements using a Quantum Design MPMS-5 superconducting quantum interference device magnetometer with an external field of 200 G.

## III. RESULTS AND DISCUSSION

### A. Chemical composition and x-ray diffraction analysis

As obtained from EDX, the typical chemical compositions of Cu:Sn:Se samples used for the electrical and optical studies were 28.6:14.5:56.9 atomic percentage, very close to the ideal value 2:1:4. However, there is a slight excess of Sn with respect to Cu (Cu/Sn≈1.97) and of cations over Se (metal/Se≈0.76). The x-ray powder pattern of $Cu_2SnSe_4$ is shown in Fig. 1. The indexing of the XRD data was performed by means of the computer program DICVOL91.[13] The ten peak positions measured from the XRD pattern were used as input data. A unique solution was readily obtained in a cubic system with unit cell parameter $a=5.6846(3)$ Å. The entire XRD pattern was reviewed by using the program *NBS*AIDS83*,[14] in the cubic space group $F\bar{4}3m$. Table I shows the XRD data for $Cu_2SnSe_4$, which included the de Wolff, $M_N$,[15] and Smith–Snyder, $F_N$,[16] figures of merit. The $Cu_2SnSe_4$ structure can be described as derivative of the zinc blende where Zn atoms are replaced by Cu, and Sn atoms, and the cationic vacancy. The atomic positions are given in Table II.

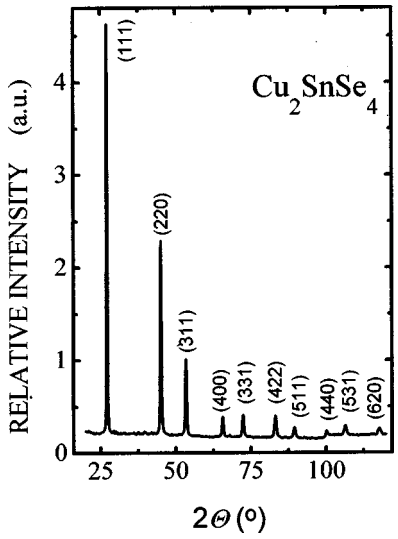


FIG. 1. XRD powder pattern of $Cu_2SnSe_4$. Values of $(h,k,l)$ for each diffraction line observed are indicated.

### B. Hole concentration and mobility

As checked by a thermal probe, all the samples obtained from the ingots were $p$-type conductivity. The variation of $\ln p$ of $Cu_2SnSe_4$ as a function of $10^3/T$ is shown in Fig. 2. It is observed that $p$ decreases with increasing temperature up to about 120 K. Then, it increases with $T$. The appearance of a minimum in the temperature variation of the hole concentration was also observed in $Cu_2SnSe_3$ and is indicative of impurity band conduction in the low temperature region.[7]

The increases of $p$ with $T$ in the high temperature region ($T>120$ K) is probably due to the thermal activation of a

TABLE I. Observed and calculated x-ray powder diffraction data for $Cu_2SnSe_4$. The unit cell lattice parameter is $a=5.6846(3)$ Å. Space group $F\bar{4}3m$ ($T_d^2$, No. 216), $Z=1$. The de Wolff, $M_N$, and Smith–Snyder, $F_N$, figures of merit are $M_{10}=216.9$; and $F_{10}=46.3$ (0.0015, 14), respectively.

| $2\theta_{obs}$(°) | $d_{obs}$(Å) | $(I/I_o)_{obs}$ | $hkl$ | $2\theta_{calc}$(°) | $d_{calc}$(Å) | $\Delta 2\theta$ (°) |
|---|---|---|---|---|---|---|
| 27.137 | 3.2831 | 100 | 111 | 27.147 | 3.2820 | 0.010 |
| 45.077 | 2.0095 | 34.8 | 220 | 45.070 | 2.0098 | −0.007 |
| 53.415 | 1.7138 | 16.5 | 311 | 53.410 | 1.7140 | −0.005 |
| 65.677 | 1.4204 | 4.9 | 400 | 65.639 | 1.4211 | −0.038 |
| 72.418 | 1.3039 | 5.1 | 331 | 72.402 | 1.3041 | −0.016 |
| 83.189 | 1.1603 | 4.9 | 422 | 83.181 | 1.1604 | −0.008 |
| 89.499 | 1.0941 | 3.3 | 511 | 89.508 | 1.0940 | 0.009 |
| 100.098 | 1.0048 | 2.9 | 440 | 100.080 | 1.0049 | −0.018 |
| 106.540 | 0.9611 | 3.6 | 531 | 106.569 | 0.9609 | 0.029 |
| 117.942 | 0.8989 | 3.3 | 620 | 117.954 | 0.8988 | 0.012 |

TABLE II. Atomic coordinates of the $Cu_2SnSe_4$ compound in the $F\bar{4}3m$ space group.

| Atom | Site | $x$ | $y$ | $z$ | foc |
|---|---|---|---|---|---|
| Cu | 4*a* | 0 | 0 | 0 | 0.50 |
| Sn | 4*a* | 0 | 0 | 0 | 0.25 |
| □[a] | 4*a* | 0 | 0 | 0 | 0.25 |
| Se | 4*c* | $\frac{1}{4}$ | $\frac{1}{4}$ | $\frac{1}{4}$ | 1.0 |

[a]Cation vacancy.

shallow acceptor level. In this case, for nearly uncompensated conductivity, the hole concentration in the valence band $p_v$ is given by the expression[17]

$$p_v(T) \approx A(T)\exp(-E_A/2K_BT), \tag{1}$$

where $E_A$ is the thermal impurity-to-valence band activation energy and $A$ a parameter which varies slowly with $T$.

To estimate $E_A$ from the $p(T)$ curve, the variation of $p$ between 120 and 300 K was analyzed by using Eq. (1). A linear plot of $\ln p$ vs $10^3/T$, as shown in Fig. 2, was observed in this temperature range. From the slope of this line, the activation energy of the acceptor level is estimated to be $E_A \approx 20$ meV.

The variation of the hole mobility $\mu$ with temperature is shown in Fig. 3. It can be noted that at low temperatures $\mu$ slightly increases with increasing $T$ indicating that the holes are predominantly scattered by ionized impurities. However, at high temperatures, $\mu$ decreases with $T$ indicating that acoustic phonon scattering is the dominant process in this temperature range.

To estimate the strength of different scattering mechanisms in the valence band, $\mu$ can be calculated by using Mathiessen's rule

$$\mu^{-1} = \mu_I^{-1} + \mu_{AC}^{-1}, \tag{2}$$

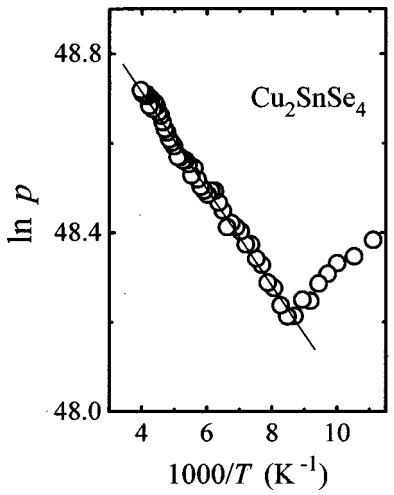


FIG. 2. Plot of $\ln p$ of $Cu_2SnSe_4$ vs $10^3/T$ in the temperature range from 80 to 300 K. The temperature variation of holes in the valence band calculated from Eq. (1) is also shown by the continuous line. From the slope of this line, the activation energy of the acceptor level is estimated to be around 20 meV.

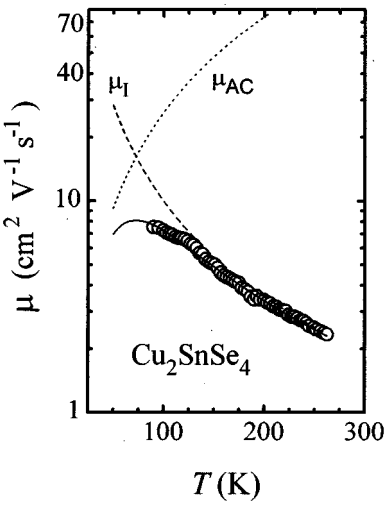


FIG. 3. Variation with temperature of the experimental hole mobility in the valence band of $Cu_2SnSe_4$. The theoretical fit to the $\mu(T)$ data, by using Eqs. (2)–(4) with the fixed parameters $\rho \approx 5.1$ g/cm$^3$, $v \approx 3.5\times10^5$ cm/s, $\epsilon_o \approx 24$, and $N_1 \approx 2\times10^{21}$ cm$^{-3}$, is shown by a continuous line. The parameters obtained from the fit were $m_{hd}^* \approx 0.8\, m_e$ and $E_{ac} \approx 30$ eV. Separate contributions to the total mobility due to ionized impurities and acoustic phonons are also shown by dotted and dashed lines, respectively.

where $\mu_I$ and $\mu_{AC}$ represent the mobilities of the charge carriers due to the scattering by ionized impurities and acoustic-lattice modes.

For $p$-type samples, the Hall mobility due to ionized impurity scattering is calculated according to the Brooks–Herring formula[18]

$$\mu_I = (2/300)2^{7/2}\epsilon_o^2(K_BT)^{3/2}[\pi^{3/2}e^3(m_{vd}^*)^{1/2}N_1 f(x)]^{-1}. \tag{3}$$

Here $\epsilon_o$ is the static dielectric constant, $m_{hd}^*$ the hole density-of-states effective mass, $N_I$ the ionized impurity concentration, and the function $f(x)$ is given by the relation $\ln(1+x) - x/(1+x)$, where $x = 6\epsilon_o m_{hd}^*(K_BT)^2/\pi e^2 h^2 p$.

The acoustical-mode scattering mobility is given by[18]

$$\mu_{AC} = (2/300)(8\pi)^{1/2}e\hbar^4\rho v^2[3E_{ac}^2(m_{hd}^*)^{5/2}(k_BT)^{3/2}]^{-1}, \tag{4}$$

where $\rho \approx 5.1$ g/cm$^3$ is the x-ray mass density, $v \approx 3.5 \times 10^5$ cm/s the longitudinal velocity of sound, and $E_{ac}$ the valence band deformation potential.

The temperature dependence of $\mu$ was fitted to Eqs. (2)–(4). In the fit, $m_{hd}^*$ and $E_{ac}$ were considered as adjustable parameters. From the electrical data, the ionized impurity concentration $N_I \approx N_A \approx p$ was estimated to be around $2 \times 10^{21}$ cm$^{-3}$. Also, from the expression $\epsilon_o^2 \propto 1/E_o$ given by Li, Anderson, and Plovnick[19] the dielectric constant was estimated to be $\epsilon_o \approx 24$, by using $E_o \approx 0.35$ eV for the energy gap, as determined from the optical data (to be discussed later). Hence, with the values of $\rho$, $v$, $N_I$, and $\epsilon_o$ given above, a good fit, as shown in Fig. 3 by continuous lines, is obtained with $m_{hd}^* \approx 0.8 m_e$ and $E_{ac} \approx 30$ eV. These values are nearly of the same order of magnitude as 1.2 $m_e$ and 21 eV, respectively, obtained[7] for $Cu_2SnSe_3$.

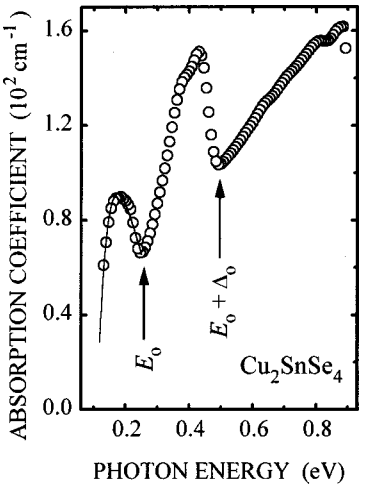


FIG. 4. Absorption coefficient spectra at room temperature of $Cu_2SnSe_4$ in the energy range from 0.1 to 0.9 eV. Optical transitions from the highest and split-off valence bands to the conduction band are indicated as $E_o$ and $E_o+\Delta_o$, respectively. The peak at around 0.18 eV is attributed to a valence band-to-acceptor level transition. The fit of the expression $\alpha\sim(h\nu-E_A)^{3/2}/(h\nu)^3$ to the data of $\alpha$ in the range from 0.10 to 0.26 eV, which gives $E_A\approx 85$ meV, is given in this figure by the continuous line.

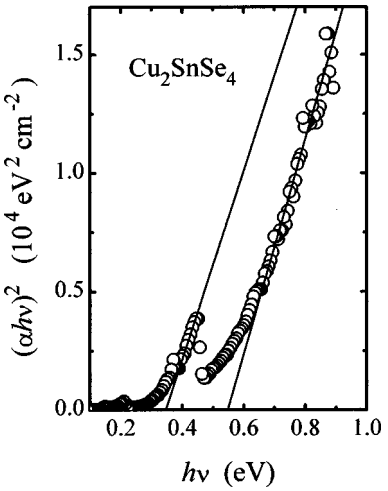


FIG. 5. Plot of $(\alpha h\nu)^2$ vs $h\nu$ of $Cu_2SnSe_a$ at room temperature in the energy range from 0.2 to 0.9 eV. From the extrapolation of the line portion of the curves to $(\alpha h\nu)^2=0$, the values $E_o\approx 0.35$ eV and $E_o+\Delta_o\approx 0.55$ eV were estimated. This gives the value $\Delta_o\approx 0.2$ eV for the spin-orbit splitting at $\mathbf{k}=0$.

### C. Optical absorption coefficient

The optical absorption coefficient was obtained from the measured transmittance through the well-known relation $\alpha=(1/t)\ln(I/I_o)-\alpha_C$, where $t$ is the thickness of the sample, $I_o$ and $I$ the intensity of the incident and transmitted light through the sample, respectively, and $\alpha_C$ is a term that accounts for the losses of the energy at the sample's surface.

Figure 4 shows the absorption coefficient spectra $\alpha$ of $Cu_2SnSe_4$ in the energy range from 0.1 to 0.9 eV at 300 K. Three absorption peaks with their maxima at about 0.18, 0.42, and 0.88 eV, are observed. In the cubic symmetry, due to the spin-orbit splitting, the threefold degenerate $p$-like $\Gamma_{15}$ valence band separates into a twofold $\Gamma_8$ and single $\Gamma_7$ bands. It is thus expected that two optical transitions from the highest doubly degenerate $\Gamma_8$ and spin-orbit split-off $\Gamma_7$ valence bands to the conduction band ($\Gamma_6$) should occur at $\mathbf{k}=0$. Thus, the last two absorption bands can be associated with these two transitions, respectively. Also, since in a direct gap semiconductor it is expected that $\alpha h\nu\sim(h\nu-E_o)^{1/2}$ for photon energy $h\nu\geqslant E_o$, to verify the nature of the band gap of $Cu_2SnSe_4$, we plot $(\alpha h\nu)^2$ as a function of $h\nu$ in Fig. 5. A linear dependence is observed for both the last two transitions indicating that $Cu_2SnSe_4$ has a direct allowed band gap at $\mathbf{k}=0$. The values $E_o\approx 0.35$ eV and $E_o+\Delta_o\approx 0.55$ eV at 300 K, were estimated by extrapolating the line portion of the curves to $(\alpha h\nu)^2=0$. This gives for the spin-orbit splitting the value $\Delta_o\approx 0.2$ eV. This is in good agreement with that calculated for $Cu_2SnSe_3$ and $Cu_2GeSe_3$ which is 0.3 and 0.24 eV, respectively.[2]

On the other hand, it was found that the narrow absorption band with the peak at about 0.18 eV follows a dependence of the form $\alpha\sim(h\nu-E_A)^{3/2}/(h\nu)^3$. This corresponds to a valence band-to-acceptor level transition[20] The fit of this expression to the data of $\alpha$ in the range from 0.10 to 0.26 eV, as also shown in Fig. 4 by the continuous line, gives $E_A\approx 85$ meV. This value is about five times higher than $E_A\approx 20$ meV estimated from electrical data. This suggests that at least two acceptor defect states are present in $Cu_2SnSe_4$. In can be also noted that in the hydrogenic approximation, the activation energy of a single shallow acceptor state can be estimated from the expression $E_{A0}\approx 13.6\,(m^*_{hd}/m_e)/\epsilon_o^2$. In the present case, using $m^*_{hd}$ and $\epsilon_o$ given above, we obtain $E_{A0}\approx 20$ meV, which coincides with the value obtained from the electrical data. This suggests that this shallow acceptor level is due to the cooper vacancy acting as a single acceptor state ($V^{1-}_{Cu}$). This identification is consistent with EDX analysis which indicates that our samples are Cu poor. On the other hand, for a double acceptor state,[21] two levels at $E_{A1}\approx 1.7\ E_{A0}\approx 35$ meV and $E_{A2}\approx 4\ E_{A0}\approx 80$ meV are expected in this compound. The last value is in good agreement with $E_A\approx 85$ meV, obtained from the optical data, indicating that this level is probably due to a double acceptor state. The possible origin of this level will be discussed in the next section.

### D. Magnetization measurements

The data of the temperature dependence of zero-field-cooled (ZFC) and field-cooled (FC) magnetization $M$ for an applied field $H=200$ G for $Cu_2SnSe_4$ are shown in Fig. 6. As observed. $M_{ZFC}$ curve slightly increases with increasing temperature, whereas $M_{FC}$ increases with decreasing $T$. This constitutes a characteristic sign of irreversible magnetic behavior and indicates that a remarkable hysteresis appears in this compound below 300 K. We have no explanation for these results at the present time. However, it is observed that both $M_{ZFC}$ and $M_{FC}$ have positive values in all the ranges of temperature studied showing that $Cu_2SnSe_4$ is paramagnetic. Because $Cu^{1+}$ should take a diamagnetic $3d^{10}$ state, it is suggested that most of the Cu atoms are divalent ($Cu^{2+}$), with $3d^9$ configuration, which should lead to a paramagnetic behavior. This is consistent with the fact that copper atoms

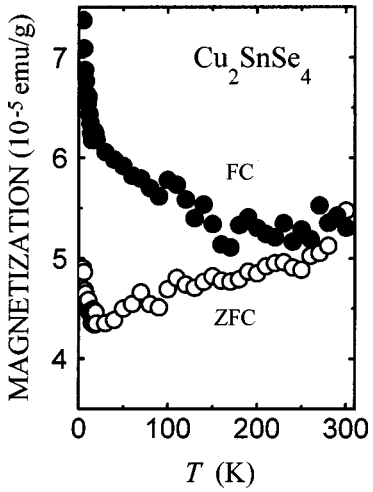


FIG. 6. Temperature dependence of the magnetization of $Cu_2SnSe_4$, for an applied field $H=200$ G, in the range from 5 to 300 K. Zero-field-cooled (ZFC) and field-cooled (FC) magnetization are indicated by open and closed circles, respectively.

should be divalent in $Cu_2SnSe_4$ in order to maintain an average of four valence electrons per lattice site. Also consistent with EDX analysis, the double acceptor level at about 80 meV can thus be explained as due to the presence of divalent copper vacancies ($V_{Cu}^{2-}$). However, the possibility that a fraction of the Cu atoms are monovalent cannot be discarded because of the presence of the shallow single acceptor level at 20 meV attributed to copper vacancies ($V_{Cu}^{1-}$). This also explains the small value of the observed susceptibility as due to the contribution of an appreciable fraction of $Cu^{1+}$ ions with a diamagnetic $3d^{10}$ state.

## IV. CONCLUSIONS

In summary, XRD study of *p*-type $Cu_2SnSe_4$ shows that this material crystallizes in a cubic structure, space group $F\bar{4}3m$, with unit cell parameter $a=5.6846(3)$ Å. From the temperature variation of hole concentration properties of this material it is found that above about 120 K, the carrier concentration is dominated by a shallow acceptor level with an activation energy of about 20 meV. The origin of this level, consistent with simple theoretical considerations for single acceptor defect states and chemical composition measurements, is tentatively assigned to single copper vacancies ($V_{Cu}^{1-}$). From the analysis of the mobility data, by assuming the scattering by acoustic phonons and ionized impurities, the density of state hole effective mass and the valence band deformation potential are calculated to be around 0.8 $m_e$ and 30 eV, respectively. On the other hand, from the optical absorption coefficient spectra at room temperature, the energy of the band gap and the spin-orbit splitting are estimated to be 0.35 and 0.2 eV, respectively. From the magnetization measurements it is found that $Cu_2SnSe_4$ is paramagnetic. This behavior is attributed to the fact that most of the copper atoms in this compound are expected to be divalent. The acceptor level of about 80 meV observed from optical data is thus attributed as due to the presence of divalent copper vacancies.

## ACKNOWLEDGMENTS

Thanks are due to Professor Juan González of the Laboratorio de Análisis Químico-Estructural de Materiales (LAQEM) for the chemical analysis and to Tec. P. Cancines of the Laboratorio de Organo-metálicos for the FTIR facilities. This work was supported by grants from CONICIT (Contract Nos. G-97000670 and LAB-97000821).

[1] L. I. Berger and V. D. Prochukhan, *Ternary Diamond-like Semiconductors* (Consultants Bureau, New York, 1969), pp. 55–63.
[2] L. K. Samanta, Phys. Status Solidi A **100**, K93 (1987).
[3] J. J. Lee, C. S. Yang, Y. S. Park, K. H. Kim, and W. T. Kim, J. Appl. Phys. **86**, 2914 (1999).
[4] M. Onoda, X. A. Chen, A. Sato, and H. Wada, Mater. Res. Bull. **35**, 1563 (2000).
[5] L. V. Piskach, O. V. Parasyuk, and Y. E. Romanyuk, J. Alloys Compd. **299**, 227 (2000).
[6] G. Marcano, D. B. Bracho, C. Rincón, G. Sánchez Pérez, and L. Nieves, J. Appl. Phys. **88**, 822 (2000).
[7] G. Marcano, C. Rincón, L. M. de Chalbaud, D. B. Bracho, and G. Sánchez Pérez, J. Appl. Phys. **90**, 1847 (2001).
[8] G. Marcano, L. M. de Chalbaud, C. Rincón, and G. Sánchez Pérez, Mater. Lett. **53**, 151 (2002).
[9] J. M. Delgado, *Ternary and Multinary Compounds 1998* (Inst. Phys. Conf. Ser. **152** 1998) (Institute of Physics, Bristol) p. 45.
[10] V. L. Bok and J. H. De Witt, Z. Anorg. Allg. Chem. **324**, 162 (1963).
[11] L. Bin, X. Yi, H. Jiaxing, and Q. Yitai, Solid State Ionics **126**, 359 (1999).
[12] Q. Li, Y. Ding, X. M. Liu, and Y. T. Qian, Mater. Res. Bull. **36**, 2649 (2001).
[13] A. Boultif and D. Louër, J. Appl. Crystallogr. **24**, 987 (1991).
[14] A. D. Mighell, C. R. Hubbard, and J. K. Stalick, National Bureau of Standards (USA), Tech. Note 1141, 1981.
[15] P. M. de Wolff, J. Appl. Crystallogr. **1**, 108 (1968).
[16] G. S. Smith and R. L. Snyder, J. Appl. Crystallogr. **12**, 60 (1979).
[17] See, for example, R. A. Smith, *Semiconductors* (Cambridge University Press, London, 1978), p. 86.
[18] D. C. Look and J. C. Manthuruthil, J. Phys. Chem. Solids **37**, 173 (1976).
[19] P. W. Li, A. R. Anderson, and R. H. Plovnick, J. Phys. Chem. Solids **40**, 333 (1979).
[20] G. Luckovsky, Solid State Commun. **3**, 105 (1965).
[21] C. Rincón and R. Márquez, J. Phys. Chem. Solids **60**, 1865 (1999).